

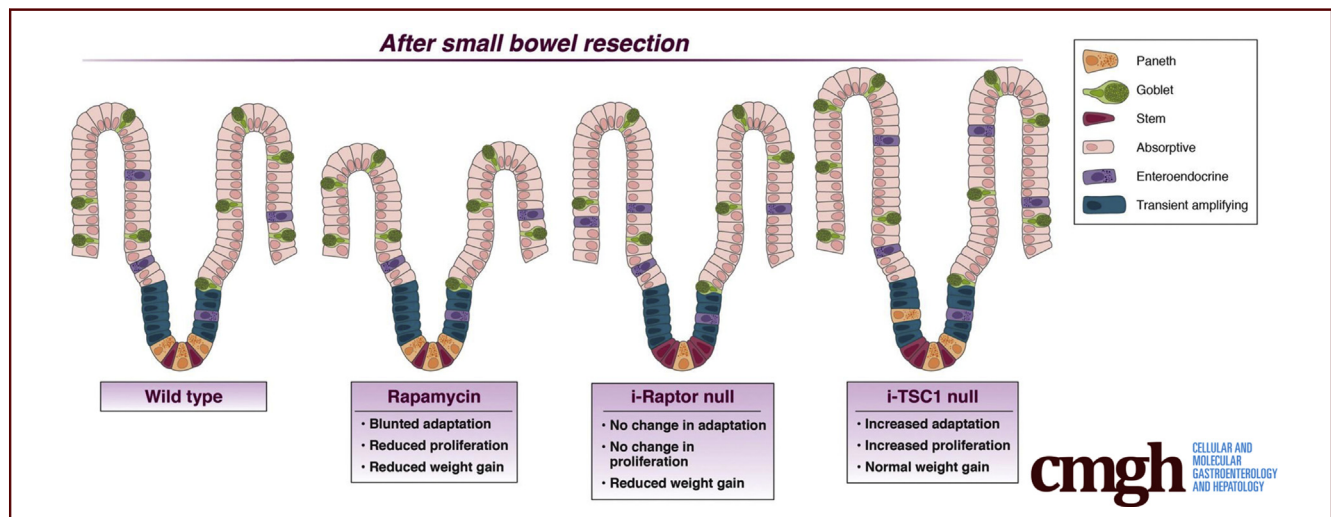
## ORIGINAL RESEARCH

## Intestinal Epithelial-Specific mTORC1 Activation Enhances Intestinal Adaptation After Small Bowel Resection



Lauren Barron, Raphael C. Sun, Bola Aladegbami, Christopher R. Erwin, Brad W. Warner, and Jun Guo

Division of Pediatric Surgery, St. Louis Children's Hospital, Department of Surgery, Washington University School of Medicine, St. Louis, Missouri



## SUMMARY

Activation of intestinal epithelial cell-specific mammalian target of rapamycin complex 1 via ablating tuberous sclerosis complex 1 enhances intestinal adaptation. Surprisingly, intestinal adaptation is not inhibited by inactivating mammalian target of rapamycin complex 1 activity in the intestinal epithelial cells, but rather by systemic inactivation via rapamycin.

**BACKGROUND & AIMS:** Intestinal adaptation is a compensatory response to the massive loss of small intestine after surgical resection. We investigated the role of intestinal epithelial cell-specific mammalian target of rapamycin complex 1 (i-mTORC1) in intestinal adaptation after massive small bowel resection (SBR).

**METHODS:** We performed 50% proximal SBR on mice to study adaptation. To manipulate i-mTORC1 activity, *Villin-Cre<sup>ER</sup>* transgenic mice were crossed with tuberous sclerosis complex (*TSC1*)<sup>flox/flox</sup> or *Raptor*<sup>flox/flox</sup> mice to inducibly activate or inactivate i-mTORC1 activity with tamoxifen. Western blot was used to confirm the activity of mTORC1. Crypt depth and villus height were measured to score adaptation. Immunohistochemistry was used to investigate differentiation and rates of crypt proliferation.

**RESULTS:** After SBR, mice treated with systemic rapamycin showed diminished structural adaptation, blunted crypt cell proliferation, and significant body weight loss. Activating i-mTORC1 via TSC1 deletion induced larger hyperproliferative crypts and disorganized Paneth cells without a significant change in villus height. After SBR, ablating TSC1 in intestinal epithelium induced a robust villus growth with much stronger crypt cell proliferation, but similar body weight recovery. Acute inactivation of i-mTORC1 through deletion of Raptor did not change crypt cell proliferation or mucosa structure, but significantly reduced lysozyme/matrix metalloproteinase-7-positive Paneth cell and goblet cell numbers, with increased enteroendocrine cells. Surprisingly, ablation of intestinal epithelial cell-specific Raptor after SBR did not affect adaptation or crypt proliferation, but dramatically reduced body weight recovery after surgery.

**CONCLUSIONS:** Systemic, but not intestinal-specific, mTORC1 is important for normal adaptation responses to SBR. Although not required, forced enterocyte mTORC1 signaling after resection causes an enhanced adaptive response. (*Cell Mol Gastroenterol Hepatol* 2017;3:231-244; <http://dx.doi.org/10.1016/j.jcmgh.2016.10.006>)

**Keywords:** TSC1; Raptor; Differentiation.

Intestinal adaptation after massive small bowel resection (SBR) is a well-established process in which the remnant bowel compensates for what has been lost.<sup>1,2</sup> Adaptation is manifested as enhanced crypt cell proliferation, deeper crypts, and taller villi, resulting in a greater mucosal surface area. How the remnant small intestine senses the postresection environmental cues to adapt remains unclear.

Mammalian target of rapamycin (mTOR) is a serine/threonine kinase that forms 2 functionally and structurally distinct complexes: mTOR complex 1 (mTORC1) and mTOR complex 2 (mTORC2).<sup>3,4</sup> mTORC1 is a well-known mediator of cell proliferation and cell growth that partners with regulatory-associated protein of mTOR (Raptor), mammalian lethal with Sec 13 protein 8/G-protein  $\beta$ -protein subunit like, Akt/Protein Kinase B (PKB) substrate 40 kilodaltons, and DEP-domain-containing mTOR interacting protein.<sup>5,6</sup> Raptor is required for mTORC1 signaling. mTORC1 activity is regulated by a variety of factors such as nutrients, growth factors, cellular stress, and energy status.<sup>7</sup> In response to growth factor stimulation, the phosphatidylinositol 3 kinase pathway is activated, which will inactivate tuberous sclerosis complex (TSC)1/2 via phosphorylation.<sup>8</sup> TSC1/2 functions to suppress mTORC1 activity by inhibiting the conversion of Rheb-guanosine diphosphate to Rheb-guanosine triphosphate.<sup>4</sup> Knockout of TSC1/2 therefore results in enhanced mTORC1 signaling. mTORC1 activation leads to phosphorylation of multiple downstream substrates such as ribosomal protein S6 kinase (S6K), translation initiation factor 4E binding proteins, unc-51 like autophagy activating kinase 1/2 (ULK1/2), and autophagy-related gene 13 (ATG13), which activate anabolic processes such as protein synthesis, lipid synthesis, and ribosomal biogenesis, while simultaneously inhibiting autophagy.<sup>4,5,7</sup>

Rapamycin is the canonical inhibitor of mTORC1 and has been used extensively for studying mTORC1 function in various tissues. In the intestine, systemic administration of rapamycin has been shown to reduce intestinal surface area in rabbits,<sup>9</sup> disrupt intestine regeneration in rats,<sup>10</sup> cause diarrhea in human beings,<sup>11</sup> and inhibit intestinal regeneration in acute inflammatory bowel disease.<sup>12</sup> Repression of mTORC1 in Paneth cells provides a niche for enhancing intestinal stem cell proliferation while keeping rates of proliferation low in transient amplifying cells.<sup>13</sup> Similar cell-specific studies have shown that activating mTORC1 in enteroendocrine L cells stimulates proglucagon promoter activity and Glucagon-like peptide-1 (GLP-1) production,<sup>14</sup> and that inhibiting mTORC1 activity in adenomatous polyposis coli (*Apc*)-deficient (Wnt-activated), but not wild-type, epithelial cells blocks crypt cell proliferation via inhibition of Eukaryotic Translation Elongation Factor 2 (eEF2) kinase activity.<sup>15</sup> Furthermore, constitutively inactivating mTORC1 in intestinal epithelium affects differentiation and compromises crypt cell regeneration after irradiation injury.<sup>16</sup>

During intestinal adaptation, the remnant small bowel mucosa faces an altered environment with different nutrients and growth factors.<sup>17,18</sup> Because mTOR can integrate a multitude of extracellular signals with intracellular cues to

regulate cell proliferation and cell growth, we hypothesized that mTOR signaling is a critical factor in adaptation. To test this hypothesis, we used rapamycin, a systemic mTOR inhibitor, to study the overall systemic role of mTOR signaling in adaptation. We then applied more sophisticated inducible and conditional genetic deletion strategies to study the function of intestinal epithelial cell-specific mTOR signaling during adaptation. Specifically, we determined the effects of SBR-induced adaptation in mice with enhanced mTORC1 signaling (inducible, intestinal epithelial cell-specific TSC1/2 knockouts) as well as in mice with attenuated mTORC1 signaling (inducible, intestinal epithelial cell-specific Raptor knockouts).

## Materials and Methods


### Mice

All protocols and experiments were approved by the Washington University Animals Studies Committee (protocol 20150285) and followed National Institutes of Health animal care guidelines. Male C57BL/6 mice, *TSC1*<sup>(flox/flox)</sup> and *Raptor*<sup>(flox/flox)</sup> mice, were purchased from the Jackson Laboratory (Bar Harbor, ME). *Villin Cre*<sup>ER</sup> mice were obtained via a generous donation from Sylvie Robine (Curie Institute, Paris, France). Intestinal epithelial-specific *TSC1* and *Raptor* knockout mice were generated by crossing *Villin Cre*<sup>ER</sup> mice with *TSC1*<sup>(flox/flox)</sup> or *Raptor*<sup>(flox/flox)</sup>, respectively. Wild-type littermates *Villin Cre*<sup>ER</sup> (-); *TSC1*<sup>(flox/flox)</sup> or *Villin Cre*<sup>ER</sup> (-); *Raptor*<sup>(flox/flox)</sup> were used as control mice. Mutant mice were maintained on a C57/BL6 background. Both male and female mice were used for small bowel resection experiments. Tamoxifen (TAM) (Sigma, St. Louis, MO) was dissolved in sunflower oil at 10 mg/mL and injected intraperitoneally at 50  $\mu$ g per gram of body weight for 3 consecutive days to induce deletion of gene expression. Mice were kept in the animal holding area with a 12-hour light-dark cycle and given rodent chow ad libitum after weaning.

### Small Bowel Resection and Harvest

The 50% proximal SBR procedure has been described previously.<sup>19</sup> The intestinal resections were performed by transecting the bowel 1- to 2-cm distal from the ligament of Treitz and at 12-cm proximal to the ileocecal junction, followed by removal of the intervening segment. Intestinal continuity was re-established by an end-to-end primary anastomosis using interrupted 9-0 monofilament sutures.

**Abbreviations used in this paper:** EGF, epidermal growth factor; IHC, immunohistochemistry; i-TSC<sup>-/-</sup>, intestinal epithelial cell-specific tuberous sclerosis complex 1 null mice; MMP, matrix metalloproteinase; mTOR, mammalian target of rapamycin; mTORC, mammalian target of rapamycin complex; PCR, polymerase chain reaction; p-HH3, phosphorylated histone H3; SBR, small bowel resection; S6K, S6 kinase; TAM, tamoxifen; TSC, tuberous sclerosis complex; WT, wild type.

 Most current article

© 2017 The Authors. Published by Elsevier Inc. on behalf of the AGA Institute. This is an open access article under the CC BY-NC-ND license (<http://creativecommons.org/licenses/by-nc-nd/4.0/>).

2352-345X

<http://dx.doi.org/10.1016/j.jcmgh.2016.10.006>

Mice were provided free access to water for the first 24 hours after surgery. Mice then were fed with a standard liquid diet (PMI Micro-Stabilized Rodent Liquid Diet LD 101; TestDiet, Richmond, IN) until death.

At the time of death, a midline laparotomy was performed and the entire small intestine was flushed with ice-cold phosphate-buffered saline containing protease inhibitors (0.2 nmol/L phenylmethylsulfonyl fluoride, 5  $\mu$ g/mL aprotinin, 1  $\mu$ mol/L benzamidine, 1 mmol/L sodium orthovanadate, and 2  $\mu$ mol/L cantharidin). A 2-cm segment of bowel distal to the anastomosis was fixed in 10% neutral-buffered formalin for histology. The remainder of the distal segment was used to isolate crypt and villus.<sup>20</sup> Protein extracted from isolated crypt or villus was used for Western blot assay, and RNA was used for real-time polymerase chain reaction (PCR) assays.

### Histology

Intestinal tissue was paraffin-embedded and cut into 5- $\mu$ m-thick longitudinal sections followed by H&E staining. Villus height and crypt depth were measured with a video-assisted computer program (NIS elements AR 4; Nikon, Melville, NY). Crypt depth was measured as the length between the bottom of the crypts and the crypt-villus junction, and villus height was determined by the length between the crypt-villi junction and the top of the villus. At least 20 well-oriented crypts and villi were counted per slide. Crypts were counted only if the crypt-villus junctions on both sides of the crypt were intact and if Paneth cells were present at the base of the crypt. Villi were counted only if the central lymphatic channel extended from the villus base to the tip and if the mucosal surface was in continuity with an intact crypt.

### Intestinal Epithelial Cell Proliferation and Differentiation Analysis

Formalin-fixed tissue sections were embedded in paraffin, sectioned, and deparaffinized. Alkaline phosphatase activity was detected via immunofluorescence using a Vector Red Alkaline Phosphatase Substrate kit (Vector Laboratories, Burlingame, CA). Secretory cell differentiation and crypt cell mitosis was detected via immunohistochemistry (IHC). Briefly, the deparaffinized slides were blocked with 3% hydrogen peroxide in methanol. Antigen retrieval was performed using Diva Decloaking solution (Biocare Medical, Concord, CA) (120°C for 2 minutes using a high-pressure cooker). Slides were blocked with avidin-pink and biotin-blue (Biocare Medical), treated with a specific antibody in DaVinci Green (Biocare Medical), incubated overnight at 4°C, and visualized with biotinylated goat anti-rabbit IgG (Jackson ImmunoResearch, Inc, West Grove, PA), followed by streptavidin-horseradish peroxidase (Jackson ImmunoResearch Laboratories, Inc, West Grove, PA), diaminobenzidine (Sigma-Aldrich, St. Louis, MO), and hematoxylin counterstaining. The antibodies used in this study were anti-p-histone H3 antibody (9701, 1:400; Cell Signaling Technology, Danvers, MA) for cell proliferation; mucin-2 (15334, 1:1000; Santa Cruz, Dallas, TX) for goblet cell differentiation; chromogranin A (20085, 1:800;

ImmunoStar, Hudson, WI) for enteroendocrine cell differentiation; matrix metalloproteinase (MMP)-7 (3801, 1:100; Cell Signaling Technology, Danvers, MA); and lysozyme (RP 028-05, 1:100; Diagnostic Biosystems, Pleasanton, CA) for Paneth cell differentiation.

### Western Blot

Isolated crypt and villus samples were lysed with sodium dodecyl sulfate sample buffer (50 mmol/L Tris-HCL, pH 6.8, 2% sodium dodecyl sulfate, 10% glycerol, and 5% mercaptoethanol). The lysate then was heated for 5 minutes at 100°C, and the protein concentration was determined using the RC-DC kit (Bio-Rad, Hercules, CA). Proteins were loaded in equal amounts for Western blot. Antibodies used in this study were as follows: TSC1 (#6935), TSC2 (#4308), Raptor (#2280), pS6K (#9234), S6K (#2708), pS6 (S235/236; #4858), pS6 (S240/244; #5364), S6 (#2217), glyceraldehyde-3-phosphate dehydrogenase (#5174), and MMP-7 (#3801) (all from Cell Signaling Technology). The proteins were detected using the Bio-Rad ChemiDoc XRS+ system with image Lab software (Bio-Rad).

### Real-Time Quantitative PCR

Isolated crypts and villi were homogenized in lysis buffer and RNA was extracted according to the manufacturer's protocol (RNAqueous kit; Ambion, Austin TX). The total RNA concentration was determined using a NanoDrop Spectrophotometer (ND-1000; NanoDrop Technologies, Wilmington, DE). TSC1, TSC2, MMP-7, and lysozyme primers were obtained from Life Technologies (Carlsbad, CA).  $\beta$ -actin was used as the endogenous control (Applied Biosystems, Foster City, CA). The Applied Biosystems 7500 Fast Real-Time PCR system was used to obtain relative RNA expression. All reverse-transcription PCR results are normalized to the  $\beta$ -actin endogenous control.

### Statistical Analysis

All values are reported as means  $\pm$  SD of the mean. Statistical analysis was performed using the Student *t* test to compare the 2 experimental groups. A *P* value less than .05 was considered significant.

## Results

### Resection-Induced Intestinal Adaptation Is Blunted by Rapamycin

To determine whether mTORC1 is involved in intestinal adaptation after resection, we first performed 50% proximal SBR on male C57BL/6 mice followed by systemic inhibition of mTORC1 via rapamycin. Small bowel resection is a major abdominal surgery with a significant physiological impact on the mice in the first 48 hours after surgery. In addition, we see a significant decrease in oral intake during this period despite the rapid regeneration process occurring at the molecular level.<sup>19</sup> Rapamycin injections have a much smaller, but similar, effect on oral intake and frailty in the mice. When these 2 procedures are compounded, the post-surgery survival rate decreases sharply. To accommodate,

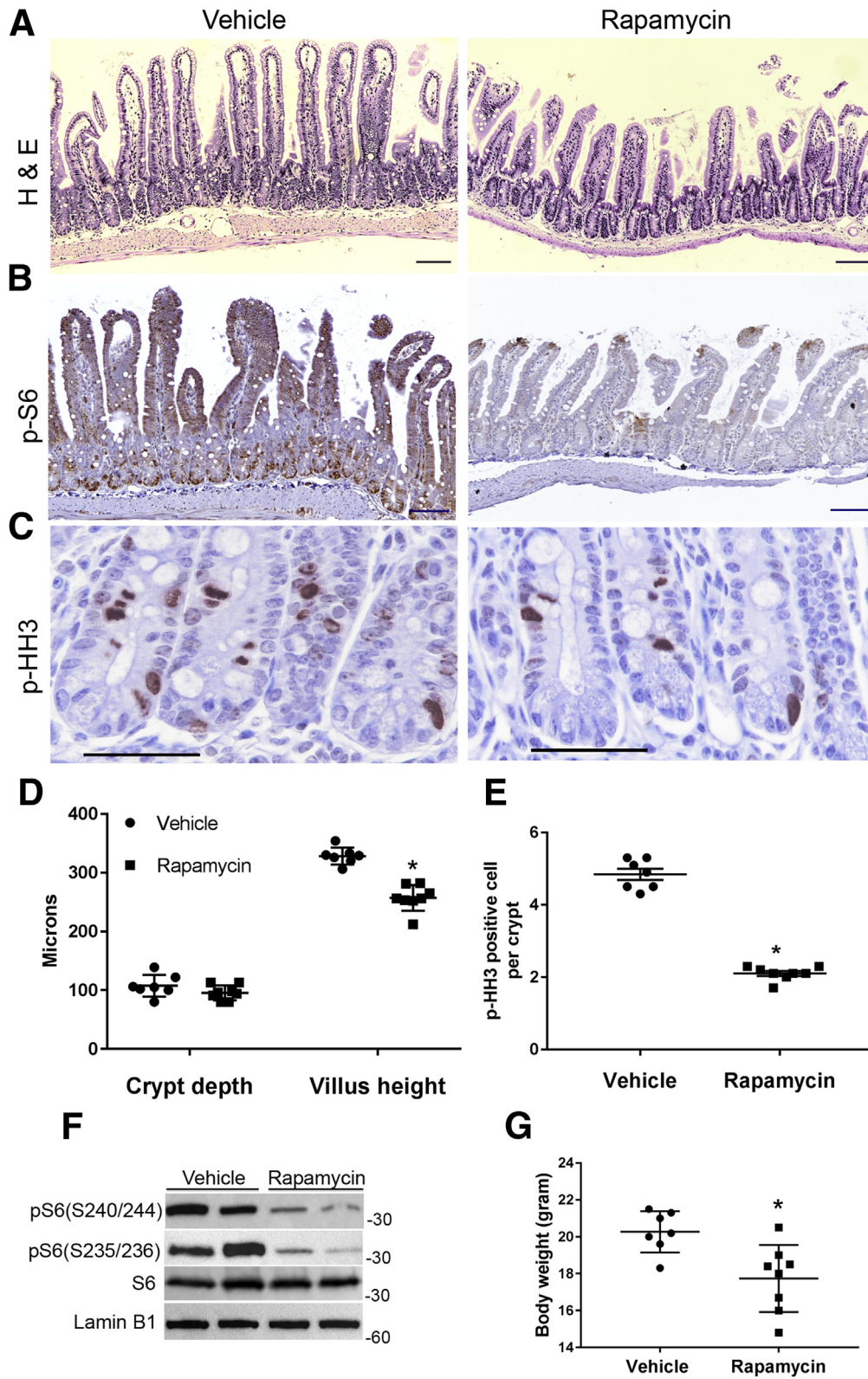


**Figure 1. Intestinal adaptation, crypt cell proliferation, and postsurgical weight gain are inhibited by rapamycin.** Eight-week-old C57BL/6 male mice were subjected to 50% proximal SBR and treated with either vehicle or rapamycin for 7 days. (A) Representative H&E staining of small intestine 7 days after SBR (n = 7 for vehicle and n = 8 for rapamycin). Scale bars: 100  $\mu$ m. (B) Representative IHC staining of p-S6 (S235/236) as a surrogate of mTORC1 activity (n = 7 per group). Scale bars: 100  $\mu$ m. (C) Representative IHC staining of p-HH3 as a mitosis marker (n = 7 for vehicle and n = 8 for rapamycin). Scale bars: 50  $\mu$ m. (D) Crypt depth and villus height measurement in SBR mice after rapamycin treatment. (E) Average number of p-HH3-positive cells per crypt. (F) Representative Western blot analysis of S6 phosphorylation in isolated small intestine epithelium from vehicle or rapamycin-treated mice (n = 7 per group). Lamin B1 was used as loading control. (G) Average mice body weight at the time of harvesting. Means  $\pm$  SD are shown. Student *t* test (\**P* < .05).

we allowed the resected mice 48 hours to recover from surgery before randomization. Mice received a daily 200- $\mu$ L intraperitoneal injection of either vehicle (5% Tween-80, 5% polyethylene glycol 400 (PEG-400) in phosphate-

buffered saline) or rapamycin (dissolved in vehicle) for 1 week at a dose of 4 mg/kg. Intestinal histology was obtained to score structural adaptation. At the same time, crypts, villi, and the adjacent mesenchyme were separated for detecting

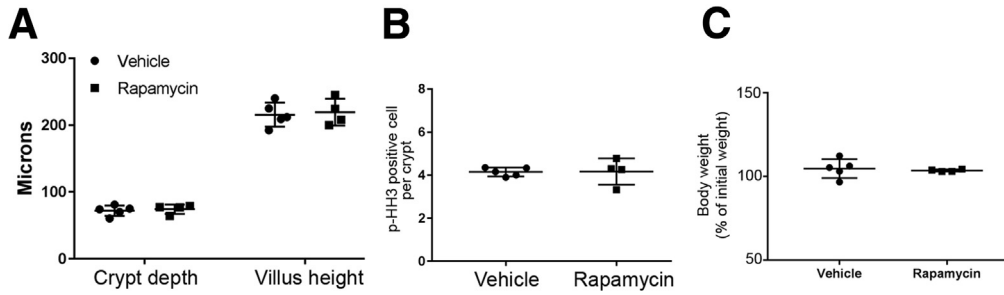


**Figure 2. Small intestine morphology and body weight are not affected by rapamycin treatment in unoperated mice.** Eight-week-old C57BL/6 male mice were subjected to either vehicle (n = 5) or rapamycin (n = 4) treatment for 7 days. (A) Crypt depth and villus height measurement after vehicle or rapamycin treatment. (B) Average number of p-HH3-positive cells per crypt. (C) Average body weight gain presented as a percentage of pretreatment weight. Means ± SD are shown. Student *t* test (*P* < .05).

mTORC1 activity in response to rapamycin inhibition. One week of rapamycin treatment resulted in a diminished adaptive response as shown by significantly decreased villus height (Figure 1A and D). Crypt cell proliferation, as measured by phosphorylated histone H3 (p-HH3, mitosis marker) IHC staining, also was decreased significantly in rapamycin-treated SBR mice (Figure 1C and E). The successful inhibition of mTORC1 activity across all layers of small intestine was confirmed by measuring phosphorylation of ribosomal protein S6, which is a common surrogate of mTORC1 activity.<sup>15,21</sup> In crypts, Western blot assay showed a dramatic decrease in ribosomal protein S6 phosphorylation at both Ser235/236 and Ser240/244, indicating decreased mTORC1 signaling (Figure 1F). Because S6

phosphorylation is similar at Ser235/236 and Ser240/244, only Ser235/236 phosphorylation was recorded for subsequent experiments. IHC staining of small intestine with pS6 antibody confirmed a significant reduction of pS6 signal in rapamycin-treated mice (Figure 1B). When body weight was measured, rapamycin-treated mice weighed significantly less when compared with vehicle-treated mice (Figure 1G). These data indicate that systemic mTORC1 signaling is important for crypt cell proliferation and adaptation after SBR.

To determine whether the effects of rapamycin inhibition were specific for the adapting bowel, we also treated unoperated C57BL/6 mice with the same dose of rapamycin for the same time period. Rapamycin treatment of these mice did not affect intestinal structure, crypt cell

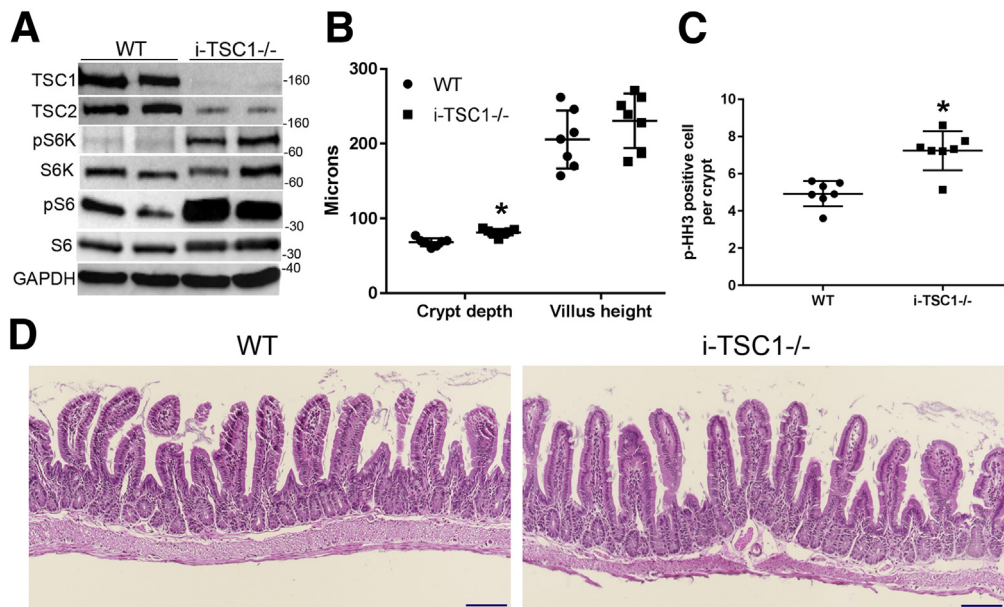


**Figure 3. Acute deletion of TSC1 in intestinal epithelium activates mTORC1 signaling and promotes crypt cell proliferation.** Villin Cre<sup>ER</sup> (-); TSC1<sup>(flox/flox)</sup> (WT) or Villin Cre<sup>ER</sup> (+); TSC1<sup>(flox/flox)</sup> (i-TSC1<sup>-/-</sup>) mice were injected intraperitoneally with tamoxifen for 3 days and small intestine was removed 2 weeks later. (A) Representative Western blot analysis confirms the deletion of TSC1 and mTORC1 activation (n = 7 per genotype). Glyceraldehyde-3-phosphate dehydrogenase (GAPDH) was used as loading control. (B) Crypt depth and villus height measurement of WT or TSC1-deficient mice (i-TSC1<sup>-/-</sup>). (C) Crypt cell proliferation was determined by the number of mitotic cells per crypt, measured by IHC staining using anti-p-HH3 antibody. (D) Representative H&E staining of small intestine 14 days after TAM injection (n = 7 per genotype). Scale bars: 100 μm. Means ± SD are shown. Student *t* test (\**P* < .05).

proliferation, or weight gain (Figure 2). These findings verify that the mTORC1 signaling pathway is involved specifically in the resection-induced adaptation process.

### *mTORC1 Activation in Intestinal Epithelium Promotes Adaptation After Resection*

Although treatment of mice with rapamycin showed that systemic mTORC1 signaling is critical for intestinal adaptation after massive SBR, our ultimate goal was to enhance adaptation responses after SBR. Because of the ubiquitous nature of mTORC1 signaling throughout the body, tissue-specific contributions to adaptation may require targeted mTORC1 activation. Because adaptation is believed to be an event involving stimulated rates of enterocyte proliferation,<sup>22</sup> we focused on genetic manipulation of intestinal epithelial cells. When bred with Rosa26 reporter mouse line, the *Villin Cre<sup>ER</sup>* line has been shown to target intestinal stem cells after TAM injection.<sup>23</sup> We therefore crossed the *Villin Cre<sup>ER</sup>* transgenic mouse with the *TSC1<sup>(flox/flox)</sup>* mouse line to generate inducible intestinal epithelial cell-specific *TSC1* null mice (i-TSC1<sup>-/-</sup>). When mice reached 6–8 weeks of age, TAM was injected intraperitoneally for 3 consecutive days. After 2 weeks, the distal ileum was excised and the deletion

of *TSC1* in i-TSC1<sup>-/-</sup> mice was confirmed by real-time PCR using isolated epithelial cells (data not shown). Western blot then was used to verify the efficient deletion of *TSC1* protein (Figure 3A). As expected, in *TSC1*-deficient epithelial cells, the well-established mTORC1 kinase target S6K and S6 were highly phosphorylated. In addition, protein expression of *TSC2*, the binding partner of *TSC1*, was degraded (Figure 3A). In contrast, *TSC1* protein expression in smooth muscle was not changed in i-TSC1<sup>-/-</sup> mice (data not shown). These results confirm that we successfully established an inducible intestinal epithelial cell-specific mTORC1 activation system for further characterization of mTORC1 signaling in the gut. When crypt depth and villus height were measured, a small, yet significant, increase (17.6%) in crypt depth was seen in unoperated i-TSC1 null mice (Figure 3B and D). The villus height, however, was not changed (Figure 3B and D). When the paraffin-embedded slides were stained with p-HH3-specific antibody to measure crypt cell proliferation, we found 34% more mitotically active crypt cells in i-TSC1 null mice (Figure 3C).

The literature shows several differing approaches to determine the role of mTORC1 in intestinal epithelial cell differentiation. However, these studies have yielded many

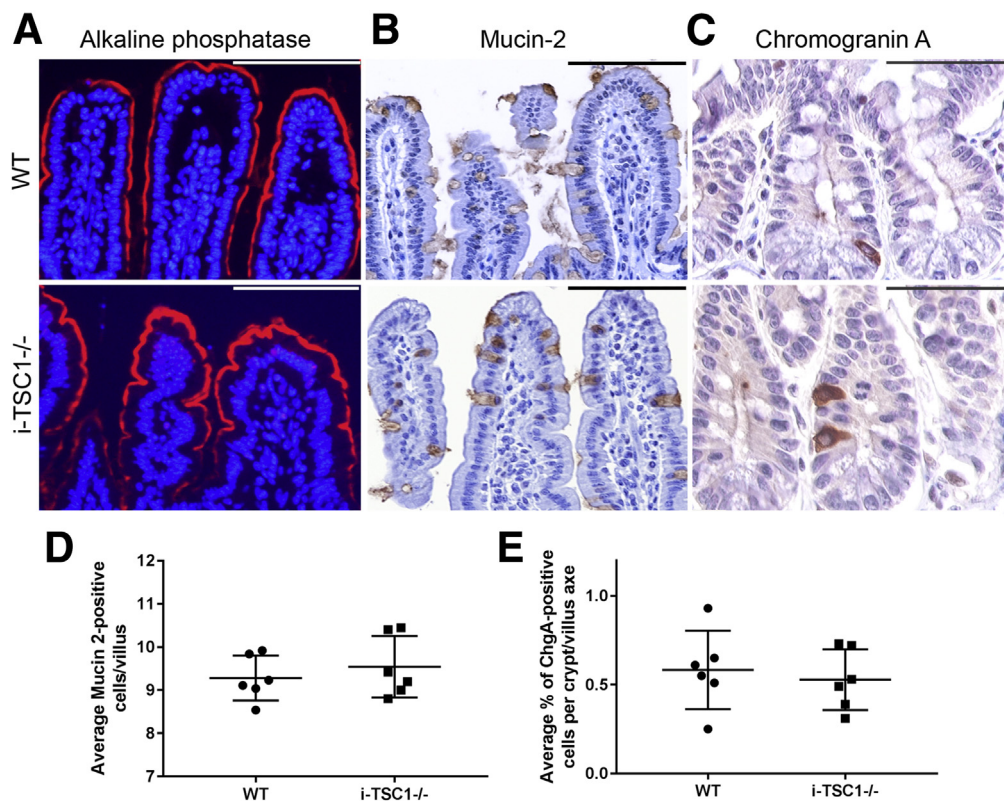


**Figure 4. The effects of *TSC1* deletion on intestinal epithelial cell differentiation.** *Villin Cre<sup>ER</sup>* (-); *TSC1<sup>(flox/flox)</sup>* (WT) or *Villin Cre<sup>ER</sup>* (+); *TSC1<sup>(flox/flox)</sup>* (i-TSC1<sup>-/-</sup>) mice underwent intraperitoneal injection with tamoxifen for 3 days and small intestine was removed 2 weeks later. (A) Representative immunofluorescence staining shows alkaline phosphatase in red (n = 6 per genotype). (B) Representative IHC shows goblet cells in brown using anti-mucin 2 antibody (n = 6 per genotype). (C) Representative IHC shows enteroendocrine cells in brown using anti-chromogranin A (ChgA) antibody (n = 6 per genotype). (D) Quantification of goblet cells based on at least 30 well-orientated villi. (E) Quantification of enteroendocrine cells based on at least 100 crypt/villus axis. Nuclei are stained with either (A) 4',6-diamidino-2-phenylindole or (B and C) hematoxylin. Scale bars: (A and B) 100  $\mu$ m, and (C) 50  $\mu$ m. Means  $\pm$  SD are shown. Student *t* test (*P* < .05).

different results based on the approach used.<sup>16,21</sup> Systemic inhibition of mTOR or Raptor has been shown to diminish the activity of alkaline phosphatase.<sup>16</sup> In this study, we found no change in alkaline phosphatase activity within villi between wild-type (WT) and *i-TSC1*<sup>-/-</sup> small intestine (Figure 4A), which indicates normal absorptive cell lineage differentiation in the absence of TSC1. Secretory cell differentiation was investigated (Paneth, goblet, and enteroendocrine cells) with IHC staining using lysozyme, mucin-2, and chromogranin A, respectively. We found that mTORC1 activation through TSC1 ablation in epithelial cells had no effect on differentiation of goblet and enteroendocrine cells (Figure 4B–E). Because Paneth cell turnover time is much longer (3 to ~8 weeks) than other cell lineages,<sup>24–26</sup> we investigated the long-term (4 weeks) effects of TSC1 deficiency on Paneth cells. Lysozyme-positive Paneth cells in WT mice showed a typical clustered pattern on the bottom of the crypt base. However, lysozyme-positive cells in *i-TSC1*<sup>-/-</sup> crypts were less uniform, yet remained confined to the crypt compartment (Figure 5A). Despite the aberrant location of lysozyme-positive cells, the mRNA level of lysozyme was not changed (Figure 5D). Lysozyme is one

of many antimicrobial peptides within the granules of Paneth cells.<sup>27</sup> To see whether TSC1 affects the overall Paneth cells, H&E-stained small intestine was examined. Indeed, the granule-containing Paneth cells often were not clustered on the bottom of *i-TSC1*<sup>-/-</sup> crypts (Figure 5B). To further delineate the effects of TSC1 deficiency on Paneth cell function, a metalloproteinase (MMP-7) that regulates intestinal  $\alpha$ -defensin activation was measured.<sup>27–29</sup> Similar to lysozyme staining, MMP-7-positive Paneth cells also clustered on the bottom of WT crypts, but were disorganized in TSC1-deficient crypts (Figure 5C). The expression level of MMP-7 protein as shown via Western blot assay was not affected in TSC1-deficient crypts (Figure 5E). These data indicate that acute activation of mTORC1 in adult mice affects crypt cell proliferation and Paneth cell organization, whereas goblet, enteroendocrine, and absorptive cell lineage differentiation remain undisturbed.

Next, we sought to investigate whether the increased proliferation seen with increased mTORC1 activation would promote structural adaptation after SBR. This study was designed to test whether acute enhancement of mTORC1 activity may have therapeutic benefit in the postoperative

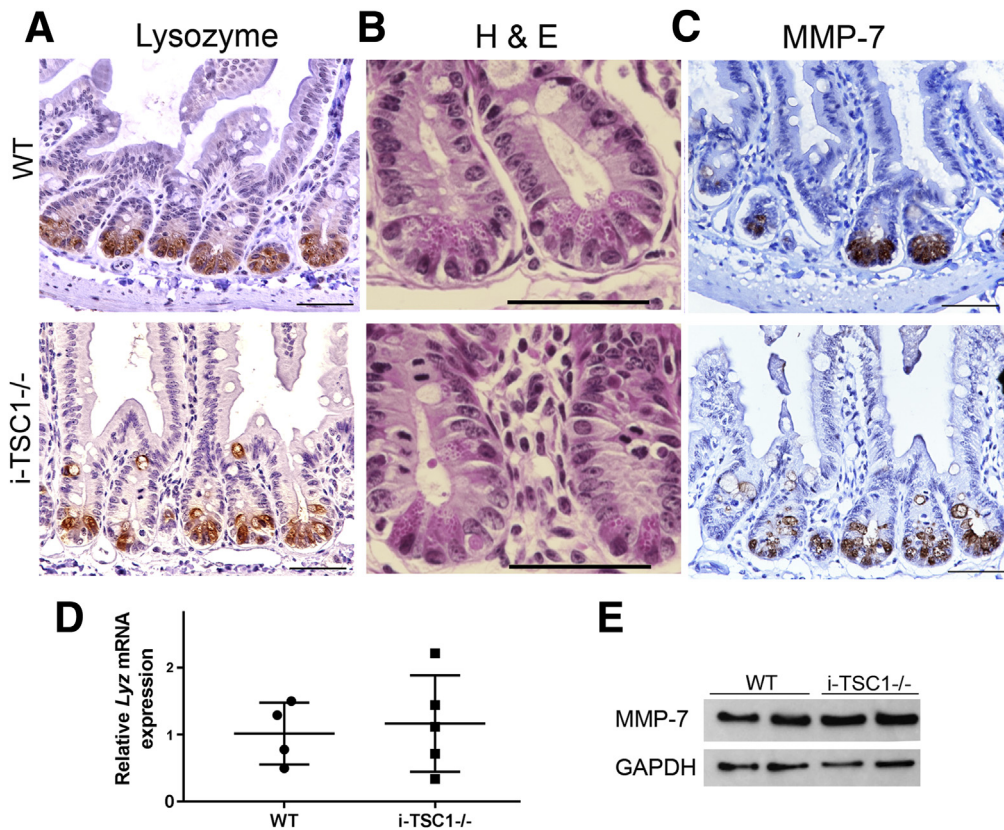


**Figure 5. The effects of TSC1 deletion on Paneth cell differentiation.** *Villin Cre<sup>ER</sup>* (-); *TSC1<sup>(flox/flox)</sup>* (WT) or *Villin Cre<sup>ER</sup>* (+); *TSC1<sup>(flox/flox)</sup>* (*i-TSC1*<sup>-/-</sup>) mice underwent intraperitoneal injection with tamoxifen for 3 days and small intestine was removed 4 weeks later. (A) Representative IHC shows Paneth cells in brown using antilysozyme antibody (n = 4 per genotype). Scale bars: 100  $\mu$ m. (B) Representative H&E staining shows Paneth cell granules in pink (n = 4 per genotype). Scale bars: 50  $\mu$ m. (C) Representative IHC shows Paneth cells in brown using anti-MMP-7 antibody (n = 4 per genotype). Scale bars: 100  $\mu$ m. (D) Reverse-transcription PCR quantification of lysozyme mRNA expression in ileal crypt cells. (E) Representative Western blot analysis of MMP-7 protein in isolated small intestinal crypt cells (n = 4 for WT and 5 for *i-TSC1*<sup>-/-</sup>). Means  $\pm$  SD are shown. Student *t* test (*P* < .05). GAPDH, glyceraldehyde-3-phosphate dehydrogenase.

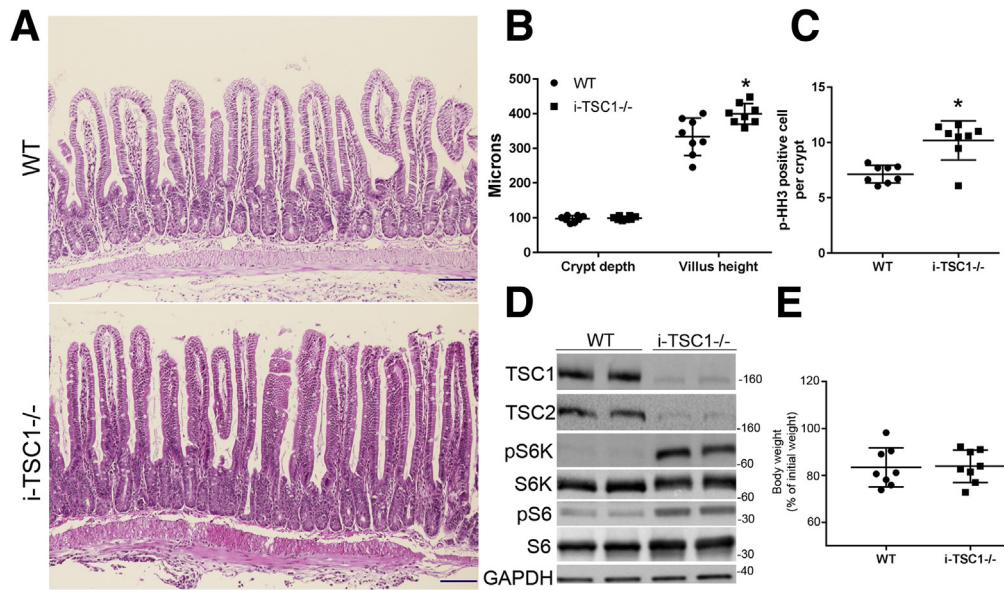


**Figure 6. Deletion of TSC1 after intestinal resection promotes adaptation and crypt proliferation.** *Villin Cre<sup>ER</sup>* (-); *TSC1<sup>(flox/flox)</sup>* (WT) or *Villin Cre<sup>ER</sup>* (+); *TSC1<sup>(flox/flox)</sup>* (i-TSC1<sup>-/-</sup>) mice underwent SBR and intraperitoneal injection with tamoxifen for 3 days. The small intestine was removed 2 weeks later. (A) Representative H&E staining of small intestine from SBR (n = 8 per genotype). Scale bars: 100 μm. (B) Crypt depth and villus height measurement of remnant ileum after resection. (C) Crypt cell proliferation was determined by the number of mitotic cells per crypt, measured by IHC staining using anti-p-HH3 antibody. (D) Western blot analysis was performed to confirm TSC1 ablation and mTORC1 activation (n = 8 per genotype). Glyceraldehyde-3-phosphate dehydrogenase (GAPDH) was used as loading control. (E) Average weight gain is presented as a percentage of preoperative weight. Means ± SD are shown. Student *t* test (\**P* < .05).

phase after massive SBR. Therefore, we performed SBR on *Villin-Cre<sup>ER</sup>* (-); *TSC1<sup>(flox/flox)</sup>* or *Villin-Cre<sup>ER</sup>* (+); *TSC1<sup>(flox/flox)</sup>* mice first. After a 2-day recovery period, we followed up with TAM injection for 3 consecutive days to activate

mTORC1 as a means of intervention during the adaptation process. The magnitude of intestinal adaptation was recorded after 2 weeks. WT mice showed a typical adaptation response although the response of the i-TSC1<sup>-/-</sup> mice was

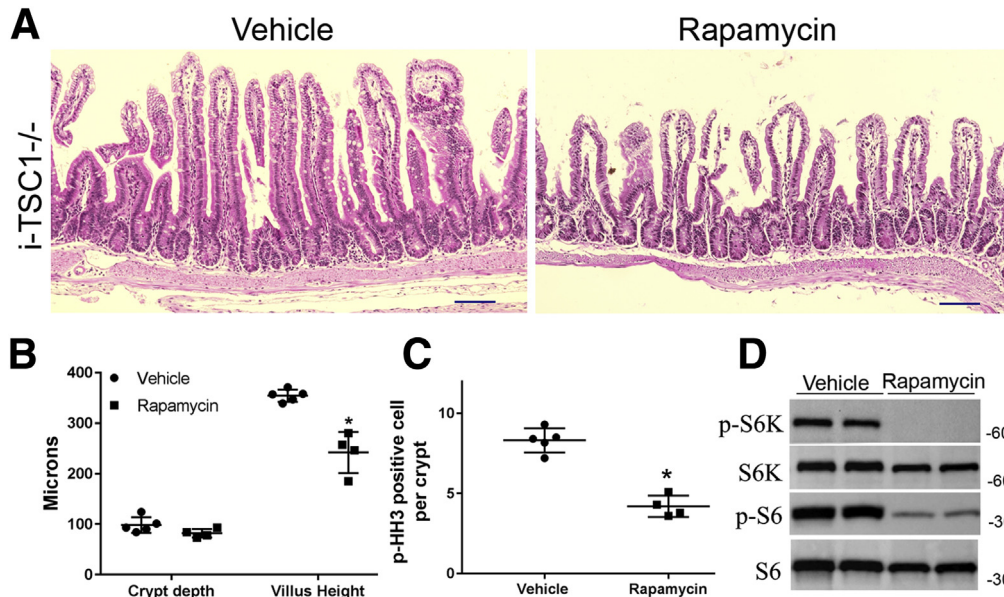


**Figure 7. mTORC1 activity accounts for TSC1-deficiency-promoted adaptation.** *Villin Cre<sup>ER</sup>* (+); *TSC1<sup>(flox/flox)</sup>* mice were injected intraperitoneally with TAM for 3 days and underwent SBR 1 week later. The resected mice were treated with either vehicle or rapamycin for 2 weeks. (A) Representative H&E staining of small intestine at the time of harvest (n = 5 for vehicle and n = 4 for rapamycin). Scale bars: 100 μm. (B) Crypt depth and villus height measurement of remnant ileum after resection. (C) Crypt cell proliferation was determined by the number of mitotic cells per crypt, measured by IHC staining using p-HH3 antibody. (D) Western blot analysis was performed to confirm rapamycin inhibition of mTORC1 activity (n = 5 for vehicle and n = 4 for rapamycin). Means ± SD are shown. Student *t* test (\**P* < .05).



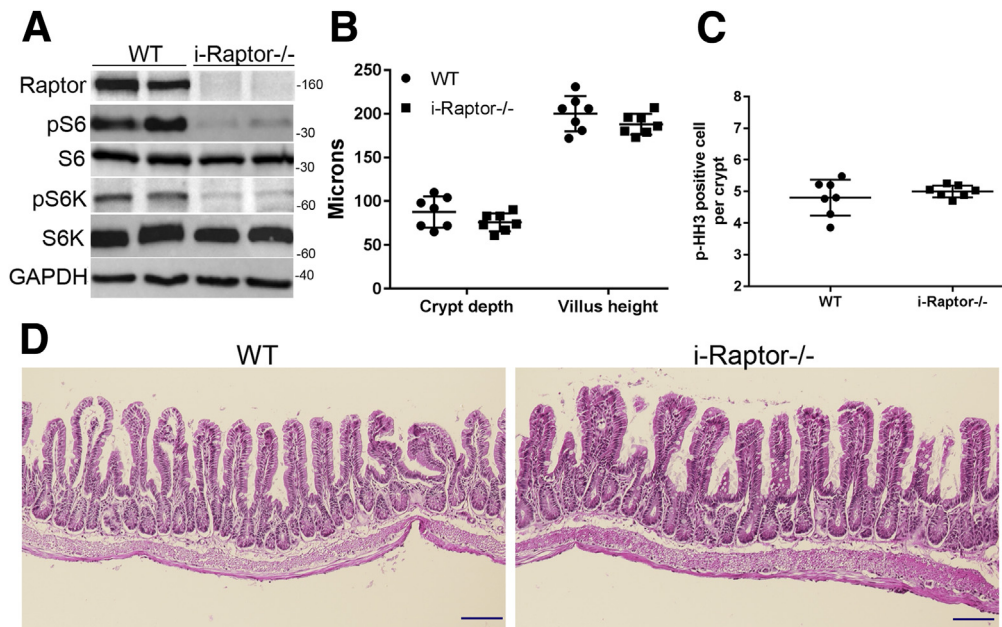


**Figure 8. Acute deletion of Raptor expression in intestinal epithelial cells does not affect small intestinal structure.** *Villin Cre<sup>ER</sup>* (-); *Raptor<sup>(flox/flox)</sup>* (WT) or *Villin Cre<sup>ER</sup>* (+); *Raptor<sup>(flox/flox)</sup>* (i-Raptor<sup>-/-</sup>) mice were injected intraperitoneally with tamoxifen for 3 days and small intestine was removed 2 weeks later. (A) Western blot analysis confirms Raptor deficiency and mTORC1 pathway inhibition (n = 7 per genotype). Glyceraldehyde-3-phosphate dehydrogenase (GAPDH) was used as loading control. (B) Crypt depth and villus height measurements of WT and Raptor-deficient mice. (C) Crypt cell proliferation was determined by the number of mitotic cells per crypt, measured by IHC using anti-p-HH3 antibody. (D) Representative H&E staining of small intestine at the time of harvest (n = 7 per genotype). Scale bars: 100  $\mu$ m. Means  $\pm$  SD are shown. Student *t* test (*P* < .05).

much stronger (~20% greater villus growth) (Figure 6A and B). Crypt proliferation in i-TSC1<sup>-/-</sup> mice, as shown by p-HH3 IHC staining, was 44% more than in the WT mice (Figure 6C). The activation of mTORC1 signaling in resected mice was confirmed by decreased TSC2 expression and increased phosphorylation of pS6 and S6K in epithelial cells (Figure 6D). Despite the increased structural intestinal adaptation, the i-TSC1<sup>-/-</sup> mice did not gain more weight than WT mice at 2 weeks after resection (Figure 6E).

We wanted to confirm that the proliferative and adaptive responses seen after SBR were owing to mTORC1 activation secondary to TSC1 inhibition rather than an alternate function of TSC1 protein. To test this, we injected mice with 3 doses of TAM to delete TSC1 first, waited for a week, and then performed SBR procedures on i-TSC1<sup>-/-</sup> mice. The modified research design was to focus on the role of TSC1 and simultaneously avoid the stress of injecting both TAM and rapamycin in postsurgical mice. After a 2-day recovery, the resected mice were randomized and treated with either vehicle or rapamycin (to inhibit mTORC1) for 2 weeks. We found that adaptation as well as resection-induced crypt cell proliferation was diminished by rapamycin treatment in i-TSC1<sup>-/-</sup> mice (Figure 7A–C). The inhibition of mTORC1 in the rapamycin-treated mice was confirmed by Western blot (Figure 7D). These data clearly verify that the enhanced proliferation and adaptation seen in TSC1-null mice after SBR is owing to the activated mTORC1 signaling pathway within intestinal epithelial cells. It also suggests that resection-induced crypt cell proliferation could be

modulated by enhancing intestinal epithelial cell mTORC1 activity.

#### *mTORC1 Inactivation in Intestinal Epithelium Does Not Affect Adaptation*

We have established that intestinal epithelial-specific activation of mTORC1 is capable of enhancing adaptation after SBR. However, it was not clear after the systemic rapamycin inhibition study whether mTORC1 signaling in intestinal epithelium is necessary for normal adaptation to occur. To investigate this, we bred *Villin Cre<sup>ER</sup>* mice with *Raptor<sup>(flox/flox)</sup>* mice to delete Raptor protein as a means of inactivating mTORC1 specifically in epithelial cells. The same experimental design in TSC1 null mice was adopted for this study. We first confirmed the deletion of Raptor protein in epithelial cells (Figure 8A). The downstream protein kinase S6K was phosphorylated at baseline but was undetectable when Raptor was deleted. In addition, pS6 phosphorylation was greatly reduced in the absence of Raptor. Despite the lack of mTORC1 signaling in the i-Raptor<sup>-/-</sup> mice, the structure of the small intestine did not change (Figure 8B and D). Rates of crypt cell proliferation were the same as in WT mice (Figure 8C), which is consistent with previously published data.<sup>15</sup> In addition, alkaline phosphatase activity was not changed, verifying that enterocyte maturation was not altered (Figure 9A). When secretory cell lineage differentiation was analyzed via IHC staining using cell differentiation specific markers, we found that goblet cells were decreased, whereas enteroendocrine

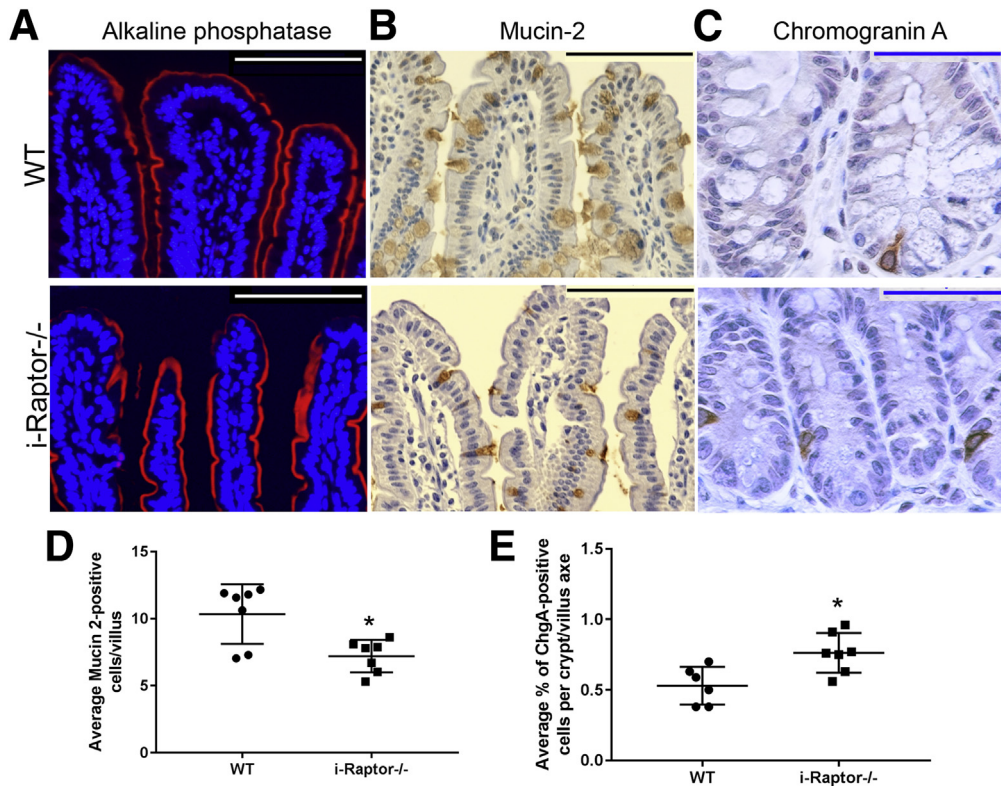


**Figure 9. Acute deletion of Raptor expression in intestinal epithelium affects differentiation.** *Villin Cre<sup>ER</sup>* (-); *Raptor<sup>flox/flox</sup>* (WT) or *Villin Cre<sup>ER</sup>* (+); *Raptor<sup>flox/flox</sup>* (i-Raptor<sup>-/-</sup>) mice underwent intraperitoneal injection with tamoxifen for 3 days and small intestine was removed after 2 weeks. (A) Representative immunofluorescence staining shows alkaline phosphatase in red (n = 7 per genotype). (B) Representative IHC shows goblet cells in brown using anti-mucin 2 antibody (n = 7 per genotype). (C) Representative IHC shows enteroendocrine cells in brown using anti-chromogranin A (ChgA) antibody (n = 7 per genotype). (D) Quantification of goblet cells based on at least 30 well-orientated villi. (E) Quantification of enteroendocrine cells based on at least 100 crypt/villus axis. Nuclei are stained with either (A) 4',6-diamidino-2-phenylindole or (B and C) hematoxylin. Scale bars: (A and B) 100  $\mu$ m, and (C) 50  $\mu$ m. Means  $\pm$  SD are shown. Student *t* test (\**P* < .05).

cells were increased in the absence of intestinal epithelial-specific Raptor (Figure 9B–E). Lysozyme-positive Paneth cells were greatly reduced after 4 weeks (Figure 10A). The granule-containing Paneth cells also were diminished in Raptor-deficient crypts in H&E-stained tissue (Figure 10B). Moreover, the expression of MMP-7 also was reduced dramatically in Raptor-deficient crypts (Figure 10C and F). Surprisingly, neither lysozyme nor MMP-7 mRNA expression levels were affected (Figure 10D and E), suggesting that Raptor protein may have a role in the translational regulation of lysozyme and MMP-7 expression during Paneth cell maturation.

Sampson et al<sup>16</sup> previously showed that mTORC1 activity is required for crypt regeneration after irradiation-induced intestinal injury. We therefore sought to determine whether mTORC1 activity is necessary for resection-stimulated crypt cell proliferation. A similar strategy was used in which SBR was performed on *Villin Cre<sup>ER</sup>* (-); *Raptor<sup>flox/flox</sup>* mice and *Villin Cre<sup>ER</sup>* (+); *Raptor<sup>flox/flox</sup>* mice. Two days after surgery TAM was given via intraperitoneal injection for 3 consecutive days to inactivate the mTORC1 pathway in the intestinal epithelium. Adaptation was analyzed 2 weeks later. Remarkably, crypt depth and villus height in i-Raptor<sup>-/-</sup> mice was the same as in WT mice

(Figure 11A and B). Crypt cell proliferation, as measured by p-HH3 IHC, also was not changed (Figure 11C). Blocked mTORC1 signaling in Raptor-deficient mice was confirmed (Figure 11D). Despite the normal structural adaptation, the Raptor-deficient mice had significantly more weight loss after surgery than the WT mice (Figure 11E).

In summary, our results show that mTORC1 activity in intestinal epithelial cells is not required for crypt proliferation and has different effects on enterocyte differentiation. Furthermore, resection-induced crypt proliferation and intestinal adaptation requires systemic, but not intestinal epithelial-specific, mTORC1 activity. However, stimulation of mTORC1 in intestinal epithelium increases crypt cell proliferation, which further enhances adaptation after SBR (Figure 12). The long-term functional significance of manipulating mTORC1 signaling in intestinal epithelial cells after small bowel resection remains unclear and will require further studies.

## Discussion

The mTOR signaling pathway has been studied extensively because it is a master regulator of cell proliferation, growth, and metabolism.<sup>3,4,6,30</sup> Historically, the majority of

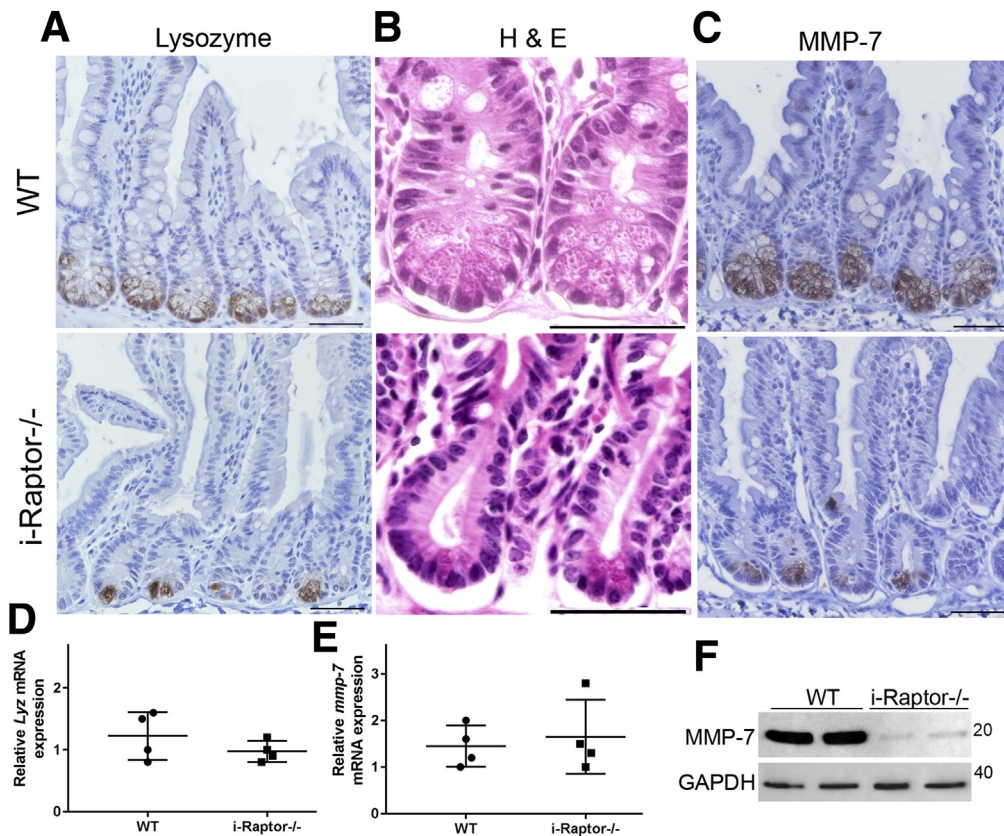


**Figure 10. The effects of Raptor deletion on Paneth cell differentiation.** *Villin Cre<sup>ER</sup>* (-); *Raptor<sup>flox/flox</sup>* (WT) or *Villin Cre<sup>ER</sup>* (+); *Raptor<sup>flox/flox</sup>* (i-Raptor<sup>-/-</sup>) mice underwent intraperitoneal injection with tamoxifen for 3 days, small intestine was removed 4 weeks later. (A) Representative IHC shows Paneth cells in brown using antilysozyme antibody (n = 4 per genotype). Scale bars: 100 μm. (B) Representative H&E staining shows Paneth cell granules in pink (n = 4 per genotype). Scale bars: 50 μm. (C) Representative IHC shows Paneth cells in brown using anti-MMP-7 antibody (n = 4 per genotype). Scale bars: 100 μm. (D) Reverse-transcription PCR quantification of lysozyme mRNA expression in ileal crypt cells. (E) Reverse-transcription PCR quantification of *MMP-7* mRNA expression in ileal crypt cells. (F) Representative Western blot analysis of *MMP-7* protein in isolated small intestine epithelium (n = 4 per genotype). Means ± SD are shown. Student *t* test (*P* < .05). GAPDH, glyceraldehyde-3-phosphate dehydrogenase.

these studies were based in cell culture. However, more recently, studies have emerged with tissue/organ-specific research that has shown varied physiological functions of mTOR in adult tissues and during development.<sup>12,13,15,16,31</sup> In intestinal tissue, several groups have used various strategies to manipulate mTOR signaling and have yielded dissimilar results. For example, using a similar strategy to constitutively delete mTOR protein specifically in intestinal epithelial cells,<sup>11,16</sup> one group clearly showed a dilated small bowel with a reduced body weight.<sup>11</sup> On the other hand, another group found that the mTOR-deficient mice have a shorter small bowel but a similar body weight.<sup>16</sup>

There is also some controversy regarding the role of mTOR signaling in intestinal cell differentiation. One report found that intestinal epithelial-specific mTOR signaling is required for proper lysozyme transcription in Paneth cells.<sup>16</sup> However, other studies found that mTOR activation via a constitutive systemic *TSC2* mutation also impaired lysozyme expression in Paneth cells.<sup>21</sup> By using an inducible Cre system to manipulate mTOR signaling in adult intestinal epithelial cells, we found that Paneth cell differentiation was

indeed regulated by mTORC1 signaling in intestinal epithelial cells, but via a different mechanism. mTORC1 inactivation does not inhibit lysozyme or *MMP-7* transcription, rather, it appears to regulate lysozyme or *MMP-7* translation. Activating mTORC1 in intestinal epithelium, on the other hand, appears to affect Paneth cell clustering on the base of crypts. Maturation of enterocytes also has been found to be disrupted in mTOR or Raptor-deficient cells based on alkaline phosphatase activity.<sup>16</sup> In our acute ablation model, we did not see any alteration in the expression of alkaline phosphatase in Raptor- or *TSC*-deficient mice. These seemingly conflicting studies may be explained by the different methods used in each study to manipulate mTOR signaling and may represent different aspects of regulation during enterocyte differentiation. In the *TSC2* mutant model,<sup>21</sup> mTORC1 activation caused by loss of the functional *TSC2* was not confined to the intestine. The mesenchyme, as well as other tissues, also would show mTORC1 activity, confounding the autonomous role of mTOR in intestinal epithelial cells. In the enterocyte mTOR-deficient model,<sup>16</sup> villin Cre was activated from embryonic

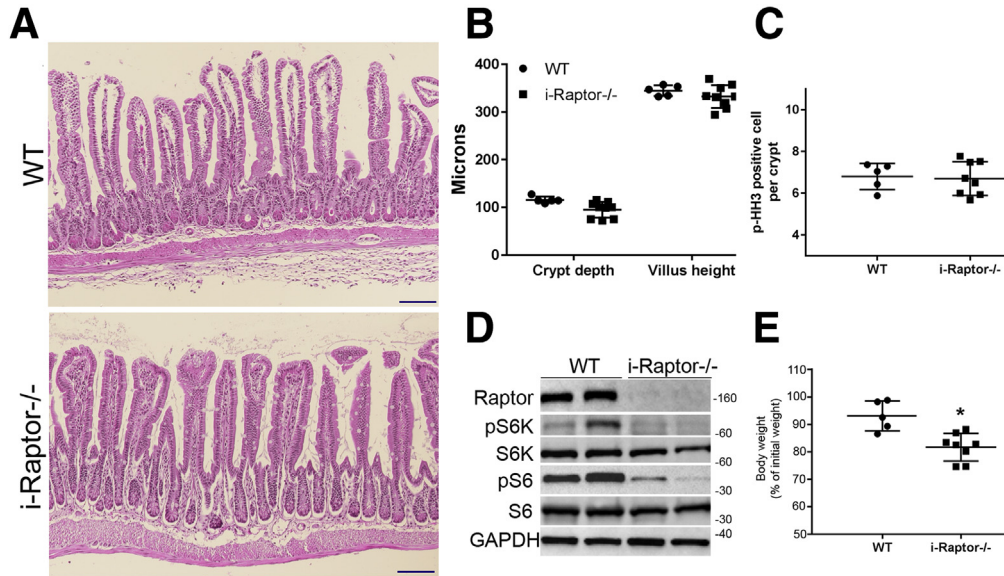


**Figure 11. Deletion of Raptor expression in intestinal epithelium after small bowel resection does not affect adaptation.** *Villin Cre<sup>ER</sup>* (-); *Raptor<sup>(flox/flox)</sup>* (WT) or *Villin Cre<sup>ER</sup>* (+); *Raptor<sup>(flox/flox)</sup>* (i-Raptor<sup>-/-</sup>) mice underwent 50% SBR, followed by intraperitoneal injection with tamoxifen for 3 days and small intestine was removed 2 weeks later. (A) Representative H&E staining of small intestine at the time of harvest (n = 5 for WT and 8 for i-Raptor<sup>-/-</sup>). Scale bars: 100 μm. (B) Crypt depth and villus height in remnant ileum after resection. (C) Crypt cell proliferation was determined by the number of mitotic cells per crypt, measured by IHC staining using anti-p-HH3 antibody. (D) Representative Western blot analysis was performed to confirm Raptor ablation and mTORC1 inactivation (n = 5 for WT and n = 8 for i-Raptor<sup>-/-</sup>). Glyceraldehyde-3-phosphate dehydrogenase (GAPDH) was used as loading control. (E) Average weight gain presented as the percentage of preoperative weight. Means ± SD are shown. Student *t* test (\**P* < .05).

day 12.5, which suggests that mTORC1 activity may be required during the development of Paneth cells as well as absorptive enterocyte differentiation. The multitude of differing results illustrates the complexity of the mTORC1 signaling pathway in regulating development and maintenance of the small intestine.

In this study, we investigated the role of mTORC1 during normal intestinal homeostasis as well as during the adaptive response after massive SBR. Although inactivating mTORC1 signaling in intestinal epithelium has no effect on intestinal structure or the adaptive response after resection, we found that stimulating mTORC1 resulted in enhanced crypt proliferation in adult mice. In addition, we showed that after massive SBR, adaptation and crypt proliferation were enhanced further when mTORC1 was activated in remnant small bowel. The notion that the function of mTORC1 differs during homeostasis and regeneration after injury has been established.<sup>15,16,32</sup> Constitutively ablating mTOR or Raptor

in intestinal epithelial cells has little effect on crypt cell proliferation and Wnt activity in the normal intestine. However, when mTORC1 signaling was absent, crypt regeneration after irradiation injury was compromised.<sup>16</sup> In *Apc<sup>min/+</sup>* mice, mTORC1 activity is required for Wnt-mediated intestinal polyp formation, likely via regulating the translational elongation rate.<sup>15,32</sup> Our results support the notion that mTORC1 regulates intestinal homeostasis and recovery after injury by different mechanisms. However, they also provide a clear distinction between the mechanism behind adaptation and that of Wnt-mediated crypt growth. Raptor deficiency alone is not sufficient to alter small intestine proliferation or adaptation after massive SBR, which indicates pathways other than the Wnt pathway may be crucial for regulating adaptation.

Inhibiting mTORC1 via rapamycin systemically, but not by Raptor deficiency in intestinal epithelial cells, blunted crypt cell proliferation and adaptation after SBR. It is possible that rapamycin may have other unknown targets aside from mTORC1 that regulate crypt cell proliferation. Alternatively, it must be considered that intestinal epithelial cells possess a redundant system to compensate for the loss of mTORC1 signaling to maintain proliferation and growth. However, this theory contradicts the findings that Raptor-deficient crypts do not grow into organoid outside of the intestine niche *in vitro*.<sup>15</sup> The more plausible mechanism to consider is that mTOR signals originating from the mesenchyme or the surrounding tissues play a critical role in this process, given that mTOR functions in a non-cell-autonomous manner.<sup>30</sup> The critical role of mesenchyme

mTORC1 manipulation		Intestinal adaptation	
		Villus height	Crypt mitosis
Inhibition	Systemic (Rapamycin)	↓	↓
	Intestinal epithelium (Raptor deletion)	↔	↔
Activation	Intestinal epithelium (TSC1 deletion)	↑	↑

**Figure 12. Summary of mTORC1 regulation of small-bowel adaptation after resection.**

subepithelial fibroblasts in maintaining intestinal niche function was established clearly in a recent report.<sup>33</sup> It appears that non-cell-autonomous mTORC1 signaling is crucial for the small bowel adaptive response after resection.

It is well known that nutrients and growth factors can enhance adaptation after resection.<sup>18,22,34</sup> We previously showed that a high-protein diet improves postoperative weight gain in resected mice,<sup>35</sup> an effect possibly owing to the higher glutamine levels in the high-protein diet. Glutamine has been shown to stimulate mTOR signaling and promote crypt expansion.<sup>36</sup> Our laboratory previously has shown that epidermal growth factor (EGF) treatment will increase the adaptive response after resection.<sup>37</sup> Because EGF stimulation activates phosphatidylinositol 3 kinase, it may destabilize the TSC1/TSC2 complex, causing increased mTORC1 activation and enhanced adaptation. Interestingly, we recently discovered that the intestinal epithelium-specific EGF receptor is not necessary for adaptation.<sup>38</sup> These EGF and mTORC1 studies provide a similar pattern for how adaptation might be regulated. The crypt niche is crucial to provide cues for adaptation to occur; when the cues are present, adaptation can be manipulated in an enterocyte-dependent manner.

## References

- Longshore SW, Wakeman D, McMellen M, et al. Bowel resection induced intestinal adaptation: progress from bench to bedside. *Minerva Pediatr* 2009; 61:239–251.
- O'Brien DP, Nelson LA, Huang FS, et al. Intestinal adaptation: structure, function, and regulation. *Semin Pediatr Surg* 2001;10:56–64.
- Dibble CC, Cantley LC. Regulation of mTORC1 by PI3K signaling. *Trends Cell Biol* 2015;25:545–555.
- Huang K, Fingar DC. Growing knowledge of the mTOR signaling network. *Semin Cell Dev Biol* 2014;36:79–90.
- Laplante M, Sabatini DM. mTOR signaling at a glance. *J Cell Sci* 2009;122:3589–3594.
- Sarbasov DD, Ali SM, Sabatini DM. Growing roles for the mTOR pathway. *Curr Opin Cell Biol* 2005;17:596–603.
- Kim SG, Buel GR, Blenis J. Nutrient regulation of the mTOR complex 1 signaling pathway. *Mol Cells* 2013; 35:463–473.
- Dan HC, Sun M, Yang L, et al. Phosphatidylinositol 3-kinase/Akt pathway regulates tuberous sclerosis tumor suppressor complex by phosphorylation of tuberin. *J Biol Chem* 2002;277:35364–35370.
- Dias VC, Madsen KL, Mulder KE, et al. Oral administration of rapamycin and cyclosporine differentially alter intestinal function in rabbits. *Dig Dis Sci* 1998; 43:2227–2236.
- Francavilla A, Starzl TE, Scotti C, et al. Inhibition of liver, kidney, and intestine regeneration by rapamycin. *Transplantation* 1992;53:496–498.
- Yang J, Zhao X, Patel A, et al. Rapamycin inhibition of mTOR reduces levels of the Na<sup>+</sup>/H<sup>+</sup> exchanger 3 in intestines of mice and humans, leading to diarrhea. *Gastroenterology* 2015;149:151–162.
- Guan Y, Zhang L, Li X, et al. Repression of mammalian target of rapamycin complex 1 inhibits intestinal regeneration in acute inflammatory bowel disease models. *J Immunol* 2015;195:339–346.
- Yilmaz OH, Katajisto P, Lamming DW, et al. mTORC1 in the Paneth cell niche couples intestinal stem-cell function to calorie intake. *Nature* 2012;486:490–495.
- Xu G, Li Z, Ding L, et al. Intestinal mTOR regulates GLP-1 production in mouse L cells. *Diabetologia* 2015; 58:1887–1897.
- Faller WJ, Jackson TJ, Knight JR, et al. mTORC1-mediated translational elongation limits intestinal tumour initiation and growth. *Nature* 2015;517:497–500.
- Sampson LL, Davis AK, Grogg MW, et al. mTOR disruption causes intestinal epithelial cell defects and intestinal atrophy postinjury in mice. *FASEB J* 2016; 30:1263–1275.
- Walther A, Coots A, Nathan J, et al. Physiology of the small intestine after resection and transplant. *Curr Opin Gastroenterol* 2013;29:153–158.
- McMellen ME, Wakeman D, Longshore SW, et al. Growth factors: possible roles for clinical management of the short bowel syndrome. *Semin Pediatr Surg* 2010; 19:35–43.
- Helmrath MA, VanderKolk WE, Can G, et al. Intestinal adaptation following massive small bowel resection in the mouse. *J Am Coll Surg* 1996;183:441–449.
- Guo J, Longshore S, Nair R, et al. Retinoblastoma protein (pRb), but not p107 or p130, is required for maintenance of enterocyte quiescence and differentiation in small intestine. *J Biol Chem* 2009;284:134–140.
- Zhou Y, Rychahou P, Wang Q, et al. TSC2/mTORC1 signaling controls Paneth and goblet cell differentiation in the intestinal epithelium. *Cell Death Dis* 2015;6:e1631.
- Shaw D, Gohil K, Basson MD. Intestinal mucosal atrophy and adaptation. *World J Gastroenterol* 2012; 18:6357–6375.
- el Marjou F, Janssen KP, Chang BH, et al. Tissue-specific and inducible Cre-mediated recombination in the gut epithelium. *Genesis* 2004;39:186–193.
- Cheng H, Merzel J, Leblond CP. Renewal of Paneth cells in the small intestine of the mouse. *Am J Anat* 1969; 126:507–525.
- Ireland H, Houghton C, Howard L, et al. Cellular inheritance of a Cre-activated reporter gene to determine Paneth cell longevity in the murine small intestine. *Dev Dyn* 2005;233:1332–1336.
- Clevers HC, Bevins CL. Paneth cells: maestros of the small intestinal crypts. *Annu Rev Physiol* 2013;75:289–311.
- Ouellette AJ. Paneth cells and innate mucosal immunity. *Curr Opin Gastroenterol* 2010;26:547–553.
- Wilson CL, Ouellette AJ, Satchell DP, et al. Regulation of intestinal alpha-defensin activation by the metalloproteinase matrilysin in innate host defense. *Science* 1999;286:113–117.
- Ayabe T, Satchell DP, Pesendorfer P, et al. Activation of Paneth cell alpha-defensins in mouse small intestine. *J Biol Chem* 2002;277:5219–5228.
- Albert V, Hall MN. mTOR signaling in cellular and organismal energetics. *Curr Opin Cell Biol* 2015;33:55–66.

31. Al-Awqati Q. Kidney growth and hypertrophy: the role of mTOR and vesicle trafficking. *J Clin Invest* 2015; 125:3304.
32. Fujishita T, Aoki K, Lane HA, et al. Inhibition of the mTORC1 pathway suppresses intestinal polyp formation and reduces mortality in ApcDelta716 mice. *Proc Natl Acad Sci U S A* 2008;105:13544–13549.
33. Aoki R, Shoshkes-Carmel M, Gao N, et al. Foxl1-expressing mesenchymal cells constitute the intestinal stem cell niche. *Cell Mol Gastroenterol Hepatol* 2016; 2:175–188.
34. Warner BW. The pathogenesis of resection-associated intestinal adaptation. *Cell Mol Gastroenterol Hepatol* 2016;2:429–438.
35. Sun RC, Choi PM, Diaz-Miron J, et al. High-protein diet improves postoperative weight gain after massive small-bowel resection. *J Gastrointest Surg* 2015;19: 451–457.
36. Moore SR, Guedes MM, Costa TB, et al. Glutamine and alanyl-glutamine promote crypt expansion and mTOR signaling in murine enteroids. *Am J Physiol Gastrointest Liver Physiol* 2015;308:G831–G839.
37. Chaet MS, Arya G, Ziegler MM, et al. Epidermal growth factor enhances intestinal adaptation after massive small bowel resection. *J Pediatr Surg* 1994;29: 1035–1039.
38. Rowland KJ, McMellen ME, Wakeman D, et al. Enterocyte expression of epidermal growth factor receptor is not required for intestinal adaptation in response to massive small bowel resection. *J Pediatr Surg* 2012; 47:1748–1753.

---

Received May 12, 2016. Accepted October 18, 2016.

**Correspondence**

Address correspondence to: Jun Guo, PhD, BJC Institute of Health Room 7118, 425 South Euclid Avenue, St. Louis, Missouri 63110. e-mail: guoj@wudosis.wustl.edu; fax: (314) 747-0610.

**Acknowledgment**

Portions of this study were presented at the 11th annual Academic Surgical Congress on February 3, 2016, in Jacksonville, FL.

**Conflicts of interest**

The authors disclose no conflicts.

**Funding**

Supported by the Morphology and Murine Models Cores of the Digestive Diseases Research Core Center of the Washington University School of Medicine (P30DK52574); the Children's Surgical Sciences Research Institute of the St. Louis Children's Hospital; and the National Institutes of Health/ National Institute of Diabetes and Digestive and Kidney Diseases (F32DK103490 to L.B.).